Nanoscale

RSC Publishing

PAPER

View Article Online
View Journal | View Issue

Lattice dynamics in mono- and few-layer sheets of WS_2 and WSe_2†

Cite this: *Nanoscale*, 2013, **5**, 9677

Weijie Zhao,‡[ac] Zohreh Ghorannevis,‡[ac] Kiran Kumar Amara,[b] Jing Ren Pang,[b] Minglin Toh,[d] Xin Zhang,[e] Christian Kloc,[d] Ping Heng Tan[e] and Goki Eda*[abc]

Received 13th June 2013
Accepted 5th August 2013

DOI: 10.1039/c3nr03052k

www.rsc.org/nanoscale

Thickness is one of the fundamental parameters that define the electronic, optical, and thermal properties of two-dimensional (2D) crystals. Phonons in molybdenum disulfide (MoS_2) were recently found to exhibit unique thickness dependence due to the interplay between short and long range interactions. Here we report Raman spectra of atomically thin sheets of WS_2 and WSe_2, isoelectronic compounds of MoS_2, in the mono- to few-layer thickness regime. We show that, similar to the case of MoS_2, the characteristic A_{1g} and $E_{2g}{}^1$ modes exhibit stiffening and softening with increasing number of layers, respectively, with a small shift of less than 3 cm^{-1} due to large mass of the atoms. Thickness dependence is also observed in a series of multiphonon bands arising from overtone, combination, and zone edge phonons, whose intensity exhibit significant enhancement in excitonic resonance conditions. Some of these multiphonon peaks are found to be absent only in monolayers. These features provide a unique fingerprint and rapid identification for monolayer flakes.

Introduction

Two-dimensional (2D) crystals derived from inorganic layered compounds offer a unique platform to explore fundamental condensed matter phenomena.[1] Recently, tremendous interest has focused on 2D crystals of molybdenum disulfide (MoS_2) and other members of the layered transition metal dichalcogenides (LTMDs) due to their intriguing electrical and optical properties.[2–13] A single monolayer of MoS_2 is a direct gap semiconductor with a high in-plane carrier mobility and excellent gate coupling for electrostatic control of charge carrier density.[10,11,14] Finite band gap and remarkable device performance make MoS_2 a complementary 2D material to graphene in nanoelectronics and photonics.[11,15] Further, sizable spin–orbit interaction along with broken inversion symmetry in monolayer MoS_2 allows optical access to valley degrees of freedom, demonstrating potential in novel spintronic and valleytronic devices.[4,9,16,17]

Tungsten-based LTMDs such as WS_2 and WSe_2 are isoelectronic to MoS_2 and exhibit a similar set of intriguing properties.[7,11,18–27] Their monolayer consists of an X–M–X sandwich[28] (where M and X denote transition metal and chalcogen atoms, respectively) with trigonal prismatic coordination as in MoS_2. Exfoliation of WS_2 and WSe_2 to mono- to few-layer thick sheets has been recently demonstrated by many groups.[7,18,19,21,25,26,29–33] This has led to observation of remarkable field-modulated transport with large in-plane mobility,[11,19] indirect-to-direct band gap transition upon isolation of single layers,[7,21,22,32] robust valley polarization,[25] second harmonic generation,[7] and tightly bound trions.[25] Spin–orbit interaction in these materials is substantially larger[34–39] compared to that in MoS_2 thus offering a robust platform to study spin and valley physics.

Although confinement effects on the electronic and excitonic dispersion relation in atomically thin sheets of tungsten dichalcogenides have been extensively studied to date,[21,34,39–41] little has been understood about the phonon behaviors in these 2D crystals. Lee *et al.*[42] recently reported that the phonon frequency of atomically thin MoS_2 flakes exhibits a unique thickness dependence where two characteristic Raman active modes A_{1g} and $E_{2g}{}^1$ exhibit opposite trends with the number of layers. Specifically, the A_{1g} mode, which involves the out-of-plane displacement of S atoms, is found to stiffen with increasing number of layers. In contrast, the $E_{2g}{}^1$ mode, which involves the in-plane displacement of Mo and S atoms, exhibits softening with flake thickness. Further studies[43] have shown that the shift in the A_{1g} mode can be explained by the interlayer interaction of S atoms in the neighboring planes, while

[a]*Department of Physics, National University of Singapore, 2 Science Drive 3, Singapore 117542. E-mail: g.eda@nus.edu.sg*

[b]*Department of Chemistry, National University of Singapore, 3 Science Drive 3, Singapore 117543*

[c]*Graphene Research Centre, National University of Singapore, 6 Science Drive 2, Singapore 117546*

[d]*School of Materials Science and Engineering, Nanyang Technological University, N4.1 Nanyang Avenue, Singapore 639798*

[e]*State Key Laboratory of Superlattices and Microstructures, Institute of Semiconductors, Chinese Academy of Sciences, Beijing 100083, China*

† Electronic supplementary information (ESI) available: Detailed Raman spectra obtained with three laser excitations and possible assignments of the multiphonon bands. See DOI: 10.1039/c3nr03052k

‡ These authors contributed equally to this work.

the unexpected trend of the E_{2g}^1 mode is explained by dielectric screening of long range Coulomb interactions.

Although these phonon modes in tungsten dichalcogenides were expected to follow the same trends as in MoS_2,[42,44,45] there have been conflicting reports on the thickness dependence of phonon modes in WS_2 and WSe_2 sheets in the mono- to few-layer regime.[7,22,26,31,32,46,47] For WSe_2, this is partly attributed to the lack of consensus on the assignment of the A_{1g} mode.[7,31,47] Of particular interest is the discrepancy between the experimental and the theoretical results where the latter suggest that A_{1g} and E_{2g}^1 are degenerate in WSe_2.[47] Further, behavior of multiphonon modes which contain rich information on the electronic and phonon dispersion relation[46] are largely unexplored. A detailed study of the phonon properties needs to be conducted in order to achieve valuable insight into phonon confinement effects in these intriguing 2D materials.

Here, we report detailed studies on the Raman spectra of mechanically exfoliated mono- and few-layer WS_2 and WSe_2 flakes. With the use of polarized spectroscopy, we demonstrate for both materials that the A_{1g} and E_{2g}^1 modes exhibit an opposite shift with the increasing number of layers indicating the effects of both short and long range interactions. We find that these phonon modes are degenerate in monolayer WSe_2 as predicted by theory[47] but the degeneracy is lifted in multilayers. We further discuss excitonic resonance Raman spectra for WS_2 and WSe_2 where a series of multiphonon bands are observed. We demonstrate that some of these features contain unique fingerprints of monolayer flakes.

Results and discussion

Fig. 1a shows the optical contrast or differential reflectance spectra of 3L WS_2 and WSe_2 flakes. The optical contrast is defined as $(R_{S+Q} - R_Q)/R_Q$ where R_{S+Q} and R_Q are the reflected light intensities from the quartz substrate with and without samples, respectively.[2,48] This quantity is proportional to absorbance for ultrathin samples and its spectral response can be interpreted as an absorption spectrum.[2,21,48] Characteristic excitonic absorption peaks A and B are observed along with a higher energy density of states peak C and split exciton peaks A′ and B′. The A and B excitonic absorption peaks arise from optical transitions involving a spin–orbit split valence band and degenerate conduction band at the K point of the Brillouin zone.[34,49] In this study, we investigate Raman scattering with three excitation wavelengths (472, 532, and 633 nm). The 532 nm excitation is in resonance with the B exciton peak of WS_2 and the A′ exciton peak of WSe_2. On the other hand, 473 nm excitation is roughly in resonance with the interband transition peak C for WS_2 and interband absorption continuum for WSe_2. The 633 nm excitation is in resonance with the A excitonic absorption for WS_2 and interband absorption but close to the B excitonic absorption for WSe_2. Raman features of both WS_2 and WSe_2 strongly depend on the excitation conditions due to energy dependent Raman cross section of the phonons (see ESI† for details). The absorption peaks shift slightly with flake thickness[21] but the resonance conditions remain largely unaltered.

The crystal structure of 2H-WX_2 belongs to D_{6h}^4 point group. There are 18 lattice dynamical modes at the center of the Brillouin zone (Γ point).[50–54] The irreducible representations of zone center phonons are as follows:[50,51,54]

$$\Gamma = A_{1g} + 2A_{2u} + B_{1u} + 2B_{2g} + E_{1g} + 2E_{1u} + E_{2u} + 2E_{2g}$$

The atomic displacement of the four Raman active modes A_{1g}, E_{1g}, E_{2g}^1 and E_{2g}^2 is shown in Fig. 1b. The A_{1g} mode is an

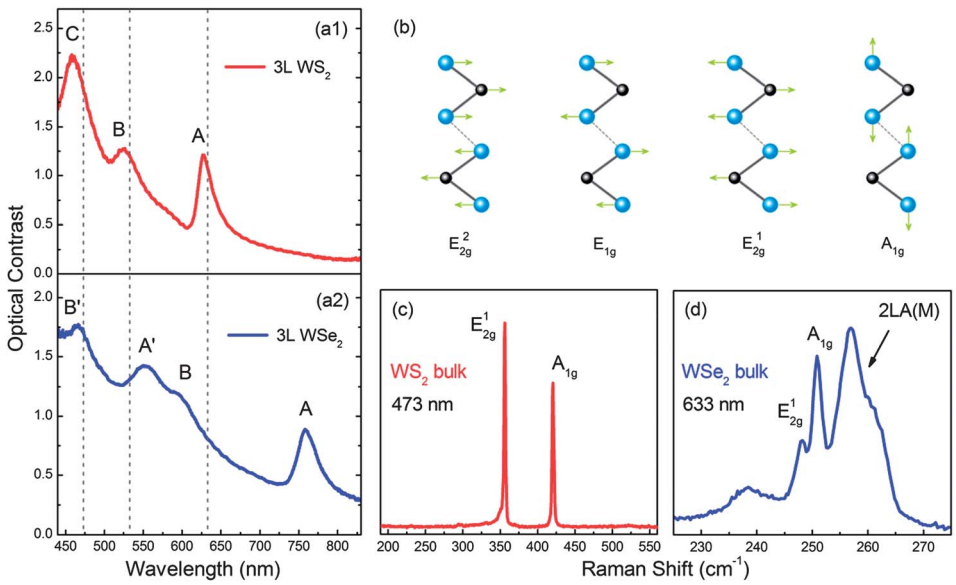

Fig. 1 Optical contrast of 3L (a1) WS_2 and (a2) WSe_2 flakes. The grey dashed arrows indicate thr wavelength of the excitation lasers used for Raman measurements. (b) Schematics showing atomic displacement of four Raman active modes in WS_2 and WSe_2. (c and d) Unpolarized Raman spectra of bulk (c) WS_2 and (d) WSe_2 obtained with 473 and 633 nm laser excitation, respectively.

out-of-plane vibration involving only the chalcogen atoms while the E_{2g}^1 mode involves in-plane displacement of transition metal and chalcogen atoms.[50,51] The E_{2g}^2 mode is a shear mode corresponding to the vibration of two rigid layers against each other and appears at very low frequencies (<50 cm^{-1}).[26,45,50,51,53,55–58] The E_{1g} mode, which is an in-plane vibration of only the chalcogen atoms, is forbidden in the back-scattering Raman configuration.[50,51]

Monolayer WX_2 belongs to the D_{3h} point group and has 9 modes at the Brillouin zone center.[43] The rigid layer shear mode E_{2g}^2 is absent in monolayers.[26,45,55,58] The unpolarized Raman spectrum of bulk WS_2 obtained with 473 nm excitation shows characteristic A_{1g} and E_{2g}^1 peaks that are clearly separated and exhibit similar intensity (Fig. 1c). In contrast, only one prominent peak is clearly seen in the bulk WSe_2 spectrum in the frequency region where we expect A_{1g} and E_{2g}^1 peaks[57] (see ESI†). In 633 nm excitation condition, however, multiple peaks are evident in this frequency region (Fig. 1d). There have been inconsistent reports on the assignment of these peaks.[7,31,32,47] We demonstrate below that two peaks found at 248 and 250 cm^{-1} are E_{2g}^1 and A_{1g} peaks in agreement with the previous study by Mead and Irwin.[57]

In polarized back-scattering Raman spectroscopy, A_{1g} mode is allowed in parallel polarization ($Z(XX)\bar{Z}$) but forbidden in cross polarization ($Z(XY)\bar{Z}$) conditions.[45] Thus the A_{1g} mode can be identified by observing Raman spectra in the two polarization conditions. Fig. 2a shows the parallel and cross polarized Raman spectra of 1 to 5L and bulk WS_2 flakes obtained with 473 nm excitation. The disappearance of the peak at ~420 cm^{-1} in cross polarization confirms that it is an A_{1g} mode. The peak at around ~356 cm^{-1} with no polarization dependence is an E_{2g}^1 mode. The peak positions agree well with the previous reports.[53,54] As shown in Fig. 2, the A_{1g} phonon stiffens and E_{2g}^1 phonon softens with increasing flake thickness similar to the case of MoS_2 (ref. 42) and as predicted by recent theoretical studies.[43] The difference in the frequency of these peaks is 60 and 65 cm^{-1} for monolayer and bulk samples, respectively (Fig. 2b). The intensity ratios (A_{1g}/E_{2g}^1) show a similar trend as seen in MoS_2. The FWHM of both peaks is found to consistently decrease with increasing number of layers (Fig. 2c).

Raman spectra of WSe_2 flakes measured in two polarization configurations and with 633 nm excitation are shown in Fig. 3a. In contrast to the case in WS_2, the parallel polarization spectra of WSe_2 flakes exhibit one prominent peak with a small shoulder in the frequency region where A_{1g} and E_{2g}^1 peaks are expected.[57] The main peak upshifts from 249.5 to 251 cm^{-1} with increasing flake thickness from monolayer to bulk. In cross polarized spectra, a single peak is observed in this frequency region. This peak is found to downshift with increasing flake thickness. The peak intensity is normalized in Fig. 3a to show this trend. The opposite thickness dependence and polarization dependence indicate that they are indeed A_{1g} and E_{2g}^1 modes. The peak at 257 cm^{-1} did not show consistent polarization dependence, as shown in the Fig. S2 of the ESI.† This peak was previously reported to be the A_{1g} phonon by some groups.[7,31,47] As shown in Fig. 1 and S2,† this peak is very broad, which is uncharacteristic for a first order Raman peak, and shows only weak dependence on the polarization configuration. This peak is assigned as the 2LA(M) phonon here according the theoretical calculation.[59] Similar to MoS_2 and WS_2, the A_{1g} (E_{2g}^1) phonon of WSe_2 stiffens (softens) with increase in flake thickness (Fig. 3b). The key difference is that the two modes become virtually degenerate in the single layer limit. We note that in 473 nm excitation conditions, only a single peak appears in the unpolarized and parallel polarized spectra due to relatively weak E_{2g}^1 peak. The general trends in FWHM and intensity ratio of A_{1g} and E_{2g}^1 peaks were consistent with those of MoS_2 and WS_2 (Fig. 3c).

Fig. 4 shows the comparison of frequencies and shifts for A_{1g} and E_{2g}^1 peaks in different Group 6 LTMDs. The E_{2g}^1 frequency

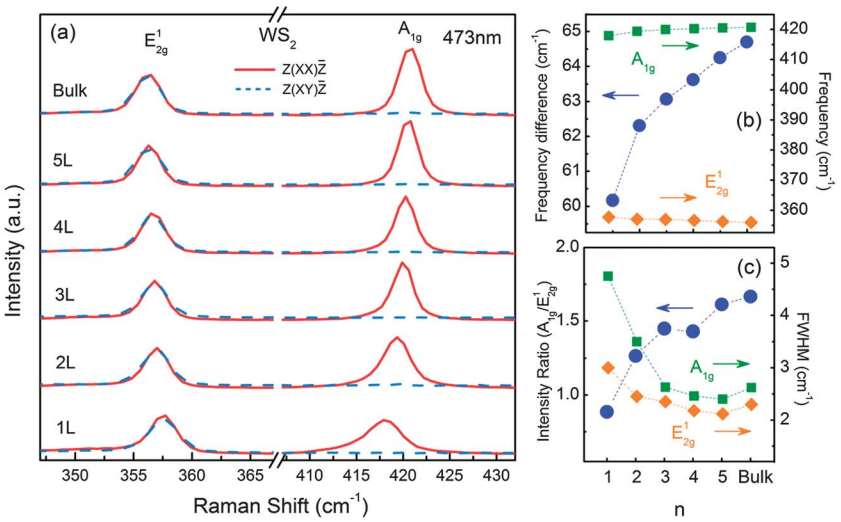

Fig. 2 (a) Raman spectra of 1 to 5L and bulk WS_2 flakes obtained in the parallel ($Z(XX)\bar{Z}$) and cross ($Z(XY)\bar{Z}$) polarization conditions with 473 nm excitation. The spectra are normalized and vertically offset for clarity. (b) Position of the A_{1g} and E_{2g}^1 modes (right vertical axis) and their difference (left vertical axis) as a function of the number of layers (n). (c) Intensity ratio (left vertical axis) and FWHM (right vertical axis) of A_{1g} and E_{2g}^1 modes as a function of the number of layers. The spectral resolution is about 0.8 cm^{-1}.

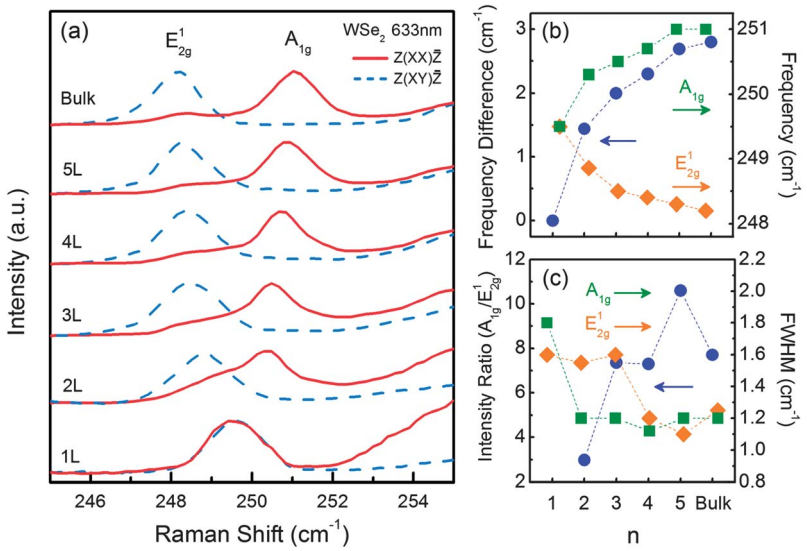

Fig. 3 (a) Raman spectra of 1 to 5L and bulk WSe_2 obtained in the parallel ($Z(XX)\bar{Z}$) and cross ($Z(XY)\bar{Z}$) polarization conditions with 633 nm excitation. The spectra are normalized and vertically offset for clarity. (b) Position of the A_{1g} and $E_{2g}{}^1$ modes (right vertical axis) and their difference (left vertical axis) as a function of the number of layers (n). (c) Intensity ratio (left vertical axis) and FWHM (right vertical axis) of A_{1g} and $E_{2g}{}^1$ modes as a function of the number of layers. The spectral resolution is about 0.2 cm^{-1}.

consistently decreases with increasing "molecular weight" of the unit cell. On the other hand, a distinct jump is found in the A_{1g} frequency between the MS_2 and MSe_2 groups. This reflects the difference in the chalcogen atomic masses. Difference in phonon frequencies between monolayer and bulk flakes (ΔA_{1g} and $\Delta E_{2g}{}^1$) is also highly dependent on the material (Fig. 4b). Stiffening and softening of the modes are most prominently observed in MoS_2 where A_{1g} and $E_{2g}{}^1$ peaks shift by 4 and 2 cm^{-1}, respectively.[42] The shift becomes less pronounced with "heavier" MX_2 with one exception of $E_{2g}{}^1$ mode of $MoSe_2$ which has been reported to exhibit a comparatively large shift (~3.6 cm^{-1}).[18] Due to the heavy atoms, WSe_2 shows the smallest thickness dependent shift (~1.3 cm^{-1}) for the two modes.

The small thickness dependence of the A_{1g} and $E_{2g}{}^1$ peaks in WS_2 and WSe_2 implies that they are not ideal fingerprints for identifying the number of layers. In the following, we discuss thickness dependence of other phonons that are observed in excitonic resonance conditions. We focus the following discussions on 532 nm resonance Raman spectra. Details of results obtained with 633 nm excitation are presented in the ESI.†

Fig. 5 and 6 show unpolarized Raman spectra obtained with 532 nm excitation, which is in resonance with B and A′ exciton absorption peaks for WS_2 and WSe_2, respectively. A series of overtone and combination peaks arising from the Brillouin zone center and zone edge phonons are observed along with the first order $E_{2g}{}^1$ and A_{1g} modes. Detailed assignments of multi-phonon bands according to recently calculated phonon dispersion curves[43,59] are summarized in Table S1 of the ESI.†

The most prominent resonance feature emerges near the $E_{2g}{}^1$ peak for both WS_2 and WSe_2. This peak, labeled as 2LA(M),

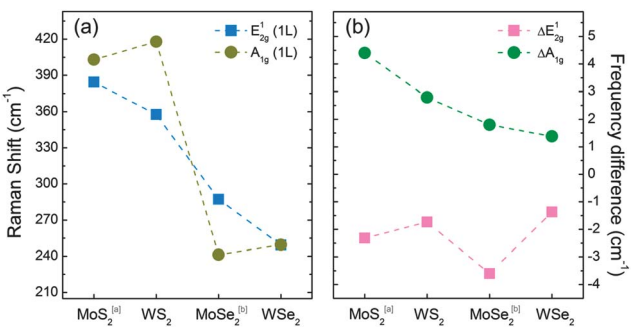

Fig. 4 (a) Frequency of the A_{1g} and $E_{2g}{}^1$ modes in monolayer MoS_2, WS_2, $MoSe_2$ and WSe_2 flakes. (b) Frequency difference (ΔA_{1g} and $\Delta E_{2g}{}^1$) between monolayer and bulk flakes for A_{1g} and $E_{2g}{}^1$ modes for the four compounds. We define ΔA_{1g} and $\Delta E_{2g}{}^1$ to be $\nu(A_{1g}(\text{bulk})) - \nu(A_{1g}(1L))$ and $\nu(E_{2g}{}^1(\text{bulk})) - \nu(E_{2g}{}^1(1L))$, respectively. The data for MoS_2 and $MoSe_2$ are obtained from ref. 42 and 18, respectively.

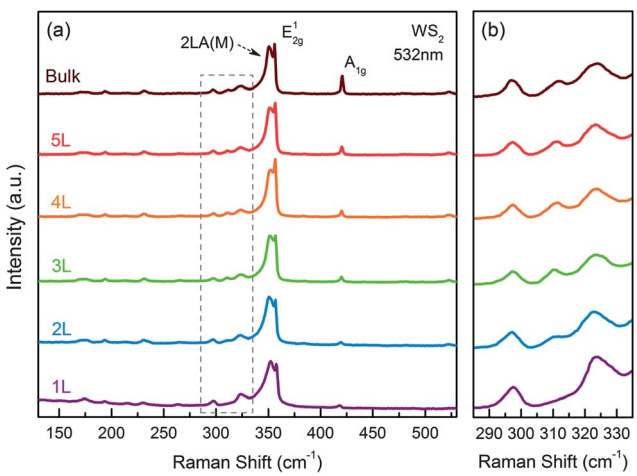

Fig. 5 (a) Unpolarized Raman spectra of 1 to 5L and bulk WS_2 flakes obtained with 532 nm excitation. The spectra are normalized to the 2LA(M) peak and vertically offset for clarity. Part of the spectra indicated by a gray dashed rectangle in (a) is shown in larger scale in (b).

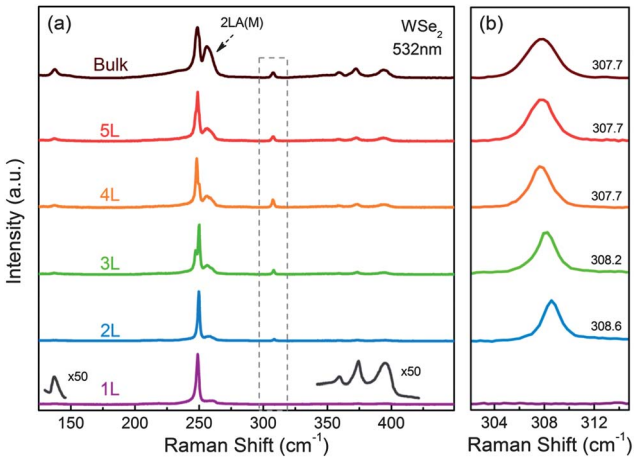

Fig. 6 (a) Unpolarized Raman spectra of 1 to 5L and bulk WSe_2 flakes obtained with 532 nm excitation. The spectra are normalized to the A_{1g} peak and vertically offset for clarity. Part of the spectra indicated by a gray dashed rectangle in (a) is shown in larger scale in (b). The numbers in (b) indicate the peak center positions.

is a second-order Raman mode due to LA phonons at the M point in the Brillouin zone.[43,54] We found that the 2LA(M) mode shows a distinct downshift of 5 cm^{-1} with increasing flake thickness from monolayer to trilayer for WSe_2 (see ESI† for details). In contrast, the same mode in WS_2 showed no obvious trend. The first-order phonon LA(M) in both WS_2 and WSe_2 is widely involved in the overtone and combination modes of other zone edge phonons, similar to the case of MoS_2.[44,60]

We observed similar multiphonon bands and 2LA(M) features with 633 nm excitation, which is in resonance with A and B exciton absorption for WS_2 and WSe_2, respectively (see ESI† for details). These results indicate that the enhancement of the total Raman cross section at excitonic resonance in which excitons serve as the intermediate state is stronger compared to that of interband resonance. The strong enhancement at excitonic resonance is attributed to the characteristics of excitons in layered materials such as large binding energy, enhanced oscillator strength, and small damping constant.[28,34,61–63] It should be noted that resonance Raman features are also seen with 473 nm excitation but to a lesser degree (see ESI† for details).

Fig. 5b highlights that a peak at ~310 cm^{-1}, which is consistently observed for multilayer flakes of WS_2, is absent in monolayers. The origin of this mode is not clear, however, its absence in monolayers suggests that it may be related to rigid layer shear mode. The relatively large frequency of this peak suggests that it is a combination of low-frequency modes.[26,45] Fig. 6b shows that similar behavior is observed in a peak located around 308 cm^{-1} for WSe_2. This peak is absent in monolayers and shows clear softening with increasing thickness. Thus, it is possibly a combination mode of a shear and E_{2g}^1 modes. Further evidence is required to verify our speculations on the origin of these peaks.

Conclusions

In summary, we study Raman scattering in mono- and few-layer WS_2 and WSe_2 flakes. Characteristic A_{1g} and E_{2g}^1 phonon modes are found to exhibit distinct thickness dependence where the former stiffens and the latter softens with increasing number of layers. While the general behavior is similar to the case of MoS_2, the thickness dependent shift of these peaks is considerably smaller for WS_2 and WSe_2 possibly due to the larger atomic masses. The A_{1g} and E_{2g}^1 modes in WSe_2 exhibit a small frequency difference in multilayers and become virtually degenerate in single layers. The presence of an E_{2g}^1 peak can be verified in cross polarized spectra where the A_{1g} mode is forbidden. Excitonic resonance Raman scattering reveals a series of multiphonon bands involving the Raman inactive phonons at Brillouin zone center and zone edge phonons. We demonstrate that some of the multiphonon bands are absent in monolayers but activated in multilayers, suggesting possible contributions from the low frequency shear modes. These features allow rapid and unambiguous identification of monolayers.

Methods

Bulk crystals of 2H-WS_2 and 2H-WSe_2 were grown by chemical vapor transport (CVT). They were mechanically exfoliated on quartz substrates and used for subsequent spectroscopic characterization. The number of layers in the flakes was confirmed by optical contrast and atomic force microscope (AFM).[21] The optical contrast spectra were measured using a tungsten–halogen lamp coupled to a Raman spectrometer. Raman spectra were acquired in ambient conditions using 473, 532 and 633 nm laser excitations. The laser power on the sample during Raman measurement was kept below 150 μW in order to avoid sample damage and excessive heating. A 2400 grooves per mm grating was used to achieve spectral resolution of below 1 cm^{-1}. The silicon Raman mode at 520 cm^{-1} was used for calibration prior to measurements.

Acknowledgements

G. Eda acknowledges Singapore National Research Foundation for funding the research under NRF Research Fellowship (NRF-NRFF2011-02). PH Tan thanks the supports from NSFC under grants 10934007 and 11225421.

References

1 K. S. Novoselov, D. Jiang, F. Schedin, T. J. Booth, V. V. Khotkevich, S. V. Morozov and A. K. Geim, Two-dimensional atomic crystals, *Proc. Natl. Acad. Sci. U. S. A.*, 2005, **102**(30), 10451–10453.

2 K. F. Mak, C. Lee, J. Hone, J. Shan and T. F. Heinz, Atomically thin MoS_2: A new direct-gap semiconductor, *Phys. Rev. Lett.*, 2010, **105**(13), 136805.

3 J. N. Coleman, M. Lotya, A. O'Neill, S. D. Bergin, P. J. King, U. Khan, K. Young, A. Gaucher, S. De, R. J. Smith, I. V. Shvets, S. K. Arora, G. Stanton, H.-Y. Kim, K. Lee, G. T. Kim, G. S. Duesberg, T. Hallam, J. J. Boland, J. J. Wang, J. F. Donegan, J. C. Grunlan, G. Moriarty, A. Shmeliov, R. J. Nicholls, J. M. Perkins, E. M. Grieveson, K. Theuwissen, D. W. McComb, P. D. Nellist and

V. Nicolosi, Two-dimensional nanosheets produced by liquid exfoliation of layered materials, *Science*, 2011, **331**(6017), 568–571.

4 K. F. Mak, K. L. He, J. Shan and T. F. Heinz, Control of valley polarization in monolayer MoS_2 by optical helicity, *Nat. Nanotechnol.*, 2012, **7**(8), 494–498.

5 A. Splendiani, L. Sun, Y. Zhang, T. Li, J. Kim, C.-Y. Chim, G. Galli and F. Wang, Emerging photoluminescence in monolayer MoS_2, *Nano Lett.*, 2010, **10**(4), 1271–1275.

6 J. S. Ross, S. Wu, H. Yu, N. J. Ghimire, A. M. Jones, G. Aivazian, J. Yan, D. G. Mandrus, D. Xiao, W. Yao and X. Xu, Electrical control of neutral and charged excitons in a monolayer semiconductor, *Nat. Commun.*, 2013, **4**, 1474.

7 H. Zeng, G. B. Liu, J. Dai, Y. Yan, B. Zhu, R. He, L. Xie, S. Xu, X. Chen, W. Yao and X. Cui, Optical signature of symmetry variations and spin-valley coupling in atomically thin tungsten dichalcogenides, *Sci. Rep.*, 2013, **3**, 1608.

8 Z. Yin, H. Li, H. Li, L. Jiang, Y. Shi, Y. Sun, G. Lu, Q. Zhang, X. Chen and H. Zhang, Single-layer MoS_2 phototransistors, *ACS Nano*, 2012, **6**(1), 74–80.

9 T. Cao, G. Wang, W. P. Han, H. Q. Ye, C. R. Zhu, J. R. Shi, Q. Niu, P. H. Tan, E. Wang, B. L. Liu and J. Feng, Valley-selective circular dichroism of monolayer molybdenum disulphide, *Nat. Commun.*, 2012, **3**, 887.

10 B. Radisavljevic, A. Radenovic, J. Brivio, V. Giacometti and A. Kis, Single-layer MoS_2 transistors, *Nat. Nanotechnol.*, 2011, **6**(3), 147–150.

11 Q. H. Wang, K. Kalantar-Zadeh, A. Kis, J. N. Coleman and M. S. Strano, Electronics and optoelectronics of two-dimensional transition metal dichalcogenides, *Nat. Nanotechnol.*, 2012, **7**(11), 699–712.

12 K. F. Mak, K. He, C. Lee, G. H. Lee, J. Hone, T. F. Heinz and J. Shan, Tightly bound trions in monolayer MoS_2, *Nat. Mater.*, 2012, **12**, 207.

13 J. Feng, X. Qian, C.-W. Huang and J. Li, Strain-engineered artificial atom as a broad-spectrum solar energy funnel, *Nat. Photonics*, 2012, **6**, 866–872.

14 J. Pu, Y. Yomogida, K.-K. Liu, L.-J. Li, Y. Iwasa and T. Takenobu, Highly flexible MoS_2 thin-film transistors with ion gel dielectrics, *Nano Lett.*, 2012, **12**(8), 4013–4017.

15 X. Song, J. Hu and H. Zeng, Two-dimensional semiconductors: recent progress and future perspectives, *J. Mater. Chem. C*, 2013, **1**(17), 2952–2969.

16 H. L. Zeng, J. F. Dai, W. Yao, D. Xiao and X. D. Cui, Valley polarization in MoS_2 monolayers by optical pumping, *Nat. Nanotechnol.*, 2012, **7**(8), 490–493.

17 G. Sallen, L. Bouet, X. Marie, G. Wang, C. R. Zhu, W. P. Han, Y. Lu, P. H. Tan, T. Amand, B. L. Liu and B. Urbaszek, Robust optical emission polarization in MoS_2 monolayers through selective valley excitation, *Phys. Rev. B: Condens. Matter Mater. Phys.*, 2012, **86**(8), 081301.

18 S. Tongay, J. Zhou, C. Ataca, K. Lo, T. S. Matthews, J. Li, J. C. Grossman and J. Wu, Thermally driven crossover from indirect toward direct bandgap in 2D semiconductors: $MoSe_2$ *versus* MoS_2, *Nano Lett.*, 2012, **12**(11), 5576–5580.

19 H. Fang, S. Chuang, T. C. Chang, K. Takei, T. Takahashi and A. Javey, High-performance single layered WSe_2 p-FETs with chemically doped contacts, *Nano Lett.*, 2012, **12**(7), 3788–3792.

20 M. M. Benameur, B. Radisavljevic, J. S. Heron, S. Sahoo, H. Berger and A. Kis, Visibility of dichalcogenide nanolayers, *Nanotechnology*, 2011, **22**(12), 125706.

21 W. Zhao, Z. Ghorannevis, L. Chu, M. Toh, C. Kloc, P.-H. Tan and G. Eda, Evolution of electronic structure in atomically thin sheets of WS_2 and WSe_2, *ACS Nano*, 2013, **7**, 791.

22 H. R. Gutiérrez, N. Perea-López, A. L. Elías, A. Berkdemir, B. Wang, R. Lv, F. López-Urías, V. H. Crespi, H. Terrones and M. Terrones, Extraordinary room-temperature photoluminescence in WS_2 monolayers, *Nano Lett.*, 2013, **13**, 3447, DOI: 10.1021/nl3026357.

23 D. J. Late, B. Liu, H. S. S. R. Matte, C. N. R. Rao and V. P. Dravid, Rapid characterization of ultrathin layers of chalcogenides on SiO_2/Si substrates, *Adv. Funct. Mater.*, 2012, **22**(9), 1894–1905.

24 H. S. S. R. Matte, B. Plowman, R. Datta and C. N. R. Rao, Graphene analogues of layered metal selenides, *Dalton Trans.*, 2011, **40**(40), 10322–10325.

25 A. M. Jones, Y. Hongyi, N. Ghimire, S. Wu, G. Aivazian, J. S. Ross, B. Zhao, J. Yan, D. Mandrus, D. Xiao, W. Yao and X. Xu, Optical generation of excitonic valley coherence in monolayer WSe_2, arXiv:1303.5318, 2013.

26 Y. Zhao, X. Luo, H. Li, J. Zhang, P. T. Araujo, C. K. Gan, J. Wu, H. Zhang, S. Y. Quek, M. S. Dresselhaus and Q. Xiong, Interlayer breathing and shear modes in few-trilayer MoS_2 and WSe_2, *Nano Lett.*, 2013, **13**(3), 1007–1015.

27 S. Horzum, H. Sahin, S. Cahangirov, P. Cudazzo, A. Rubio, T. Serin and F. M. Peeters, Phonon softening and direct to indirect band gap crossover in strained single-layer MoSe_{2}, *Phys. Rev. B: Condens. Matter Mater. Phys.*, 2013, **87**(12), 125415.

28 J. A. Wilson and A. D. Yoffe, Transition metal dichalcogenides discussion and interpretation of observed optical, electrical and structural properties, *Adv. Phys.*, 1969, **18**(73), 193.

29 G. Eda, T. Fujita, H. Yamaguchi, D. Voiry, M. Chen and M. Chhowalla, Coherent atomic and electronic heterostructures of single-layer MoS_2, *ACS Nano*, 2012, **6**(8), 7311–7317.

30 G. Eda, H. Yamaguchi, D. Voiry, T. Fujita, M. Chen and M. Chhowalla, Photoluminescence from chemically exfoliated MoS_2, *Nano Lett.*, 2011, **11**(12), 5111–5116.

31 H. Li, G. Lu, Y. Wang, Z. Yin, C. Cong, Q. He, L. Wang, F. Ding, T. Yu and H. Zhang, Mechanical Exfoliation and characterization of single- and few-layer nanosheets of WSe_2, TaS_2, and $TaSe_2$, *Small*, 2013, **9**, 1974, DOI: 10.1002/smll.201202919.

32 P. Tonndorf, R. Schmidt, P. Böttger, X. Zhang, J. Börner, A. Liebig, M. Albrecht, C. Kloc, O. Gordan, D. R. T. Zahn, S. M. d. Vasconcellos and R. Bratschitsch, Photoluminescence emission and Raman response of monolayer MoS_2, $MoSe_2$, and WSe_2, *Opt. Express*, 2013, **21**, 4908.

33 Z. Y. Zeng, Z. Y. Yin, X. Huang, H. Li, Q. Y. He, G. Lu, F. Boey and H. Zhang, Single-Layer Semiconducting nanosheets:

High-yield preparation and device fabrication, *Angew. Chem., Int. Ed.*, 2011, **50**(47), 11093–11097.
34 R. Coehoorn, C. Haas and R. A. de Groot, Electronic structure of $MoSe_2$, MoS_2, and WSe_2. II. The nature of the optical band gaps, *Phys. Rev. B*, 1987, **35**(12), 6203–6206.
35 Y. Ding, Y. Wang, J. Ni, L. Shi, S. Shi and W. Tang, First principles study of structural, vibrational and electronic properties of graphene-like MX_2 (M = Mo, Nb, W, Ta; X = S, Se, Te) monolayers, *Phys. B*, 2011, **406**(11), 2254–2260.
36 T. Cheiwchanchamnangij and W. R. L. Lambrecht, Quasiparticle band structure calculation of monolayer, bilayer, and bulk MoS_2, *Phys. Rev. B: Condens. Matter Mater. Phys.*, 2012, **85**(20), 205302.
37 A. Ramasubramaniam, Large excitonic effects in monolayers of molybdenum and tungsten dichalcogenides, *Phys. Rev. B: Condens. Matter Mater. Phys.*, 2012, **86**(11), 115409.
38 W. S. Yun, S. W. Han, S. C. Hong, I. G. Kim and J. D. Lee, Thickness and strain effects on electronic structures of transition metal dichalcogenides: 2H-MX_2 semiconductors (M = Mo, W; X = S, Se, Te), *Phys. Rev. B: Condens. Matter Mater. Phys.*, 2012, **85**(3), 033305.
39 Z. Y. Zhu, Y. C. Cheng and U. Schwingenschlögl, Giant spin–orbit-induced spin splitting in two-dimensional transition-metal dichalcogenide semiconductors, *Phys. Rev. B: Condens. Matter Mater. Phys.*, 2011, **84**(15), 153402.
40 F. Consadori and R. F. Frindt, Crystal size effects on the exciton absorption spectrum of WSe_2, *Phys. Rev. B: Solid State*, 1970, **2**(12), 4893–4896.
41 R. F. Frindt, Optical absorption of a few unit-cell layers of MoS_2, *Phys. Rev.*, 1965, **140**(2A), A536–A539.
42 C. Lee, H. Yan, L. E. Brus, T. F. Heinz, J. Hone and S. Ryu, Anomalous lattice vibrations of single- and few-layer MoS_2, *ACS Nano*, 2010, **4**(5), 2695–2700.
43 A. Molina-Sanchez and L. Wirtz, Phonons in single-layer and few-layer MoS_2 and WS_2, *Phys. Rev. B: Condens. Matter Mater. Phys.*, 2011, **84**(15), 155413.
44 B. Chakraborty, H. S. S. R. Matte, A. K. Sood and C. N. R. Rao, Layer-dependent resonant Raman scattering of a few layer MoS_2, *J. Raman Spectrosc.*, 2013, **44**, 92, DOI: 10.1002/jrs.4147.
45 X. Zhang, W. P. Han, J. B. Wu, S. Milana, Y. Lu, Q. Q. Li, A. C. Ferrari and P. H. Tan, Raman spectroscopy of shear and layer breathing modes in multilayer MoS_2, *Phys. Rev. B: Condens. Matter Mater. Phys.*, 2013, **87**, 115413.
46 A. Berkdemir, H. R. Gutierrez, A. R. Botello-Mendez, N. Perea-Lopez, A. L. Elias, C.-I. Chia, B. Wang, V. H. Crespi, F. Lopez-Urias, J.-C. Charlier, H. Terrones and M. Terrones, Identification of individual and few layers of WS_2 using Raman spectroscopy, *Sci. Rep.*, 2013, **3**, 1755.
47 H. Sahin, S. Tongay, S. Horzum, W. Fan, J. Zhou, J. Li, J. Wu and F. M. Peeters, Anomalous Raman spectra and thickness-dependent electronic properties of WSe_2, *Phys. Rev. B: Condens. Matter Mater. Phys.*, 2013, **87**(16), 165409.
48 K. F. Mak, M. Y. Sfeir, Y. Wu, C. H. Lui, J. A. Misewich and T. F. Heinz, Measurement of the optical conductivity of graphene, *Phys. Rev. Lett.*, 2008, **101**(19), 196405.
49 A. R. Beal, W. Y. Liang and J. C. Knights, Transmission spectra of some transition-metal dichalcogenides. II. Group VIA: trigonal prismatic coordination, *J. Phys. C: Solid State Phys.*, 1972, **5**(24), 3540.
50 J. L. Verble and T. J. Wieting, Lattice mode degeneracy in MoS_2 and other layer compounds, *Phys. Rev. Lett.*, 1970, **25**(6), 362–365.
51 T. J. Wieting and J. L. Verble, Infrared and Raman studies of long-wavelength optical phonons in hexagonal MoS_2, *Phys. Rev. B: Solid State*, 1971, **3**(12), 4286–4292.
52 T. Sekine, M. Izumi, T. Nakashizu, K. Uchinokura and E. Matsuura, Raman-scattering and infrared reflectance in 2H-$MoSe_2$, *J. Phys. Soc. Jpn.*, 1980, **49**(3), 1069–1077.
53 T. Sekine, T. Nakashizu, K. Toyoda, K. Uchinokura and E. Matsuura, Raman scattering in layered compound 2H-WS_2, *Solid State Commun.*, 1980, **35**(4), 371–373.
54 C. Sourisseau, F. Cruege, M. Fouassier and M. Alba, Second-order Raman effects, inelastic neutron scattering and lattice dynamics in 2H-WS_2, *Chem. Phys.*, 1991, **150**(2), 281–293.
55 G. Plechinger, S. Heydrich, J. Eroms, D. Weiss, C. Schuller and T. Korn, Raman spectroscopy of the interlayer shear mode in few-layer MoS_2 flakes, *Appl. Phys. Lett.*, 2012, **101**(10), 101906.
56 P. H. Tan, W. P. Han, W. J. Zhao, Z. H. Wu, K. Chang, H. Wang, Y. F. Wang, N. Bonini, N. Marzari, N. Pugno, G. Savini, A. Lombardo and A. C. Ferrari, The shear mode of multilayer graphene, *Nat. Mater.*, 2012, **11**(4), 294–300.
57 D. G. Mead and J. C. Irwin, Long wavelength optic phonons in WSe_2, *Can. J. Phys.*, 1977, **55**(5), 379–382.
58 H. Zeng, B. Zhu, K. Liu, J. Fan, X. Cui and Q. M. Zhang, Low-frequency Raman modes and electronic excitations in atomically thin MoS_2 films, *Phys. Rev. B: Condens. Matter Mater. Phys.*, 2012, **86**(24), 241301.
59 C. Ataca, H. Şahin and S. Ciraci, Stable, single-layer MX_2 transition-metal oxides and dichalcogenides in a honeycomb-like structure, *J. Phys. Chem. C*, 2012, **116**(16), 8983–8999.
60 H. Li, Q. Zhang, C. C. R. Yap, B. K. Tay, T. H. T. Edwin, A. Olivier and D. Baillargeat, From bulk to monolayer MoS_2: Evolution of Raman scattering, *Adv. Funct. Mater.*, 2012, **22**(7), 1385–1390.
61 M. Cardona and G. Guntherodt, Light scattering in solids II, *Top. Appl. Phys.*, 1982, **50**, 33–38; M. Cardona and G. Guntherodt, Light scattering in solids III, *Top. Appl. Phys.*, 1982, **51**, 214.
62 P. Y. Yu and M. Cardona, *Fundamentals of Semiconductors: Physics and Materials Properties*, Springer, Berlin; New York, 3rd, rev. and enlarged edn, 2001, p xviii, p. 639.
63 B. Bendow and J. L. Birman, Theory of resonant Raman scattering in crystals: A generalized bare-exciton approach, *Phys. Rev. B: Solid State*, 1971, **4**(2), 569–583.